Opto-Electronic Smart Home: Heterogeneous Optical Sensors Approaches and Artificial Intelligence for Novel Paradigms in Remote Monitoring

Arnaldo Leal-Junior, Letícia Avellar, Wilfried Blanc, Anselmo Frizera, Carlos Marques

Opto-Electronic Smart Home: Heterogeneous Optical Sensors Approaches and Artificial Intelligence for Novel Paradigms in Digital Health

Arnaldo Leal-Junior, *Member, IEEE*, Letícia Avellar, Wilfried Blanc, Anselmo Frizera, *Senior Member, IEEE*, and Carlos Marques

***Abstract*—This paper presents the development and implementation of an-optical fiber integrated smart environment with heterogeneous opto-electronic approaches. In this case, the so-called Opto-electronic Smart Home is composed of three different optical fiber sensor system, which are also based on different optical fibers, resulting in more than 50 integrated sensors. The proposed smart environment is capable of detecting the location of the patient inside the home environment, recognize patient's activities and provide the gait analysis through kinematics and spatio-temporal parameters of the gait. The heterogeneity of the system is verified by the use of the transmission-reflection analysis (TRA) using nanoparticle (NP)-doped optical fibers for the patient localization in Layer 1. Then, in Layer 2 a polymer optical fiber (POF) integrated pants is used by the patient, where the activity detection, especially walking, sitting and lying down is performed by the multiplexed intensity variation-based sensor integrated in the pants (with 30 sensors at each leg of the pants). Layer 3 comprises a fiber Bragg grating (FBG)-embedded smart carpet, where 10 FBGs are inscribed in a single mode silica optical fiber. In addition, a graphical interface is developed for the sensors integration and cloud connectivity, where the signal processing is performed using the feedforward neural network (FFNN) approach for the location of mechanical perturbation along the optical fiber (for patient localization), activity classification and footsteps location along the FBG-embedded smart carpet. The implementation results show the feasibility of the proposed system, where the location of the patients, their activities and gait analysis.**

***Index Terms*—Digital health, Distributed optical fiber sensors, Internet of Things, Photonics digitalization**

I. INTRODUCTION

THE internet of Things (IoT) is a fast growing concept of interconnection of different devices without the human intervention using the internet as the gateway [1] and, as such, there is a massive device interconnection, which leads to a high amount of data [2]. These criteria also put demands on the communication system that must be able to provide low latency and high reliability [3]. In addition, there are ever increasing demands of privacy and security on the data transmission due to its widespread in different applications, including digital health [4], industry [5], smart cities [6] and environmental monitoring [7]. As one of these applications, the digital health is a growing field that involves different novel approaches of smart homes (for remote monitoring) [8], smart healthcare for the assistance of health professionals [9] and wearable devices for continuous monitoring of patients [10]. Such smart systems present important advantages related to the remote patients monitoring, the possibility of real-time assessment of patients conditions and preventive care using sensor data in conjunction with machine learning approaches [11].

The efforts of developing integrated technologies for remote healthcare include the home instrumentation with electronic approaches and cameras as depicted in [11]. In addition, the development of wearable sensors is proposed as a viable tool for continuous monitoring of patients [12]. The possibility of connecting such wearable devices in the cloud is also an important breakthrough in digital health development as presented in [13]. It is also important to mention that the integration of different devices for a robotic physical rehabilitation approach was already proposed in [14]. However, the conjunction of heterogeneous optical sensors approaches integration for different applications, cloud-based data transmission and the artificial intelligence integration for decision-making process was not widely explored in the literature.

Among the different sensors technologies, electronic sensors are currently employed in such applications as summarized in [10]. However, the fast widespread of optical and opto-electronic systems have enable the development of numerous smart devices using optics and photonics [15]. In general, optical fiber sensors are aligned with the demands of remote healthcare not only due to their small dimensions and possibility of embedding in different structures [16], but also

This research is financed by FAPES (1004/2022 P: 2022-6PC5F, 2022-C5K3H and 458/2021), CNPq (310668/2021-2) and MCTI/FNDCT/FINEP 2784/20. C. Marques acknowledges Fundacao para a Ciencia e a Tecnologia (FCT) through the CEECIND/00034/ 2018 (iFish project) and 2021.00667.CEECIND. This work was developed within the scope of the project i3N, UIDB/50025/2020 and UIDP/50025/2020, financed by national funds through the FCT/MEC. A. Frizera acknowledges CNPq (304049/2019-0). *(Corresponding author: Arnaldo Leal-Junior).*

A. Leal-Junior, L. Avellar and A. Frizera are with Graduate Program in Electrical Engineering, Federal University of Espírito Santo (UFES), Fernando Ferrari Avenue, Vitória, 29075-910, Brazil. (e-mail: leal-junior.arnaldo@ieee.org; leticia.avellar@ufes.br; frizera@ieee.org,)

W. Blanc is with Université Côte d'Azur, Institut de Physique de Nice, CNRS, 06108 Nice Cedex 2, France (e-mail: wilfried.blanc@inphyni.cnrs.fr).

C. Marques is with I3N & Physics Department, University of Aveiro, Aveiro, 3810-193, Portugal (carlos.marques@ua.pt).

due to their unmatched multiplexing capabilities [17]. These advantages are well aligned with the development of IoT systems that require a high number of sensors and fast data transmission. For this reason, the use of optical fiber sensors heterogeneous systems for remote healthcare brings the possibility of continuous monitoring of patients activities, resulting remote assistive services, including diagnosis, early detection of health issues and their transport in case of emergencies [18].

It is worth to mention that there are many approaches for optical fiber sensors development, which include interferometers [19], gratings-based devices [20], intensity variation principle [21] and optical time (or frequency)-domain reflectometry [22]. Considering a fully instrumented smart environment with optical fiber sensors, each of these different approaches can result in particular benefits for each specific application. For example, a portable sensor can be applied for wearable monitoring of the patient [23]. In addition, distributed sensing approaches can be used on the integrated instrumentation of different regions in a smart home [24]. Moreover, the quasi-distributed sensors approaches with high spatial resolution can be embedded in different structures for smart objects with integrated optical fiber sensors [25].

Distributed optical fiber sensors systems are generally employed for long-range measurement of temperature and strain, where applications such as pipeline monitoring was already proposed [26]. As such sensors generally needs bulk and complex hardware for signal processing, distributed optical sensing approaches were proposed based on the transmission and reflection analysis (TRA) of the optical powers [27]. Recently, TRA approach benefits from the development of novel optical fibers with embedded nanoparticles (NP-doped fibers) [28], which increase the Rayleigh reflections signal and make the greatly enhances the spatial resolution in TRA approaches [27]. To that extent, distributed optical fiber sensors systems based on TRA can be used on local detection and short-range applications [29], which are aligned with the requirements of home monitoring.

Another important approach for multiplexed optical fiber sensors systems, the fiber Bragg gratings (FBGs) are conventionally used due to the possibility of inscribing numerous sensors in a single optical fiber cable with the centimeter-scale space between them [30]. However, the FBG sensors require alternative interrogation approaches or additional developments in the signal acquisition unit, since it is generally bulk and non-portable. To that extent, the multiplexing technique for intensity variation-based sensor can fill the gap or mitigate the drawbacks of FBG sensors in wearable and portable applications [31]. In this case, the technique is based on the side coupling between the optical fiber and light emitting diodes (LEDs), where the sequential activation of the LEDs result in a time-decoupled system as depicted in [32]. Thus, the multiplexed intensity variation sensors can be applied in wearable applications, including the clothing integration for continuous and real-time monitoring of patients [33].

This paper presents the integration of optical fiber sensors based on three different approaches for remote healthcare monitoring at home, namely TRA-based systems, FBGs and multiplexed intensity variation sensors. To that extent, there is not only different sensors approaches, but also different types of optical fibers, where the silica single mode optical fiber is used on the FBG sensors, the polymer optical fiber is applied in the multiplexed intensity variation sensors, whereas the NP-doped fibers are applied in the TRA approach. A 6m x 6m room, simulating a small house, is instrumented with a DNP-doped fiber and the TRA system setup is used. Moreover, an FBG-based instrumented carpet is included in this room for gait analysis with the measurement of spatial-temporal parameters and ground reaction forces. Furthermore, the person is wearing the POF Smart Pants as a wearable approach for biomechanics analysis and remote activity monitoring. Therefore, the proposed heterogeneous optical fiber sensors system is a flexible and integrated approach for the development of smart environments in Healthcare 4.0. It is also important to mention that a graphical interface with integrated deep learning algorithms is developed to perform the synchronization of the systems by the button control to start and stop the acquisition. The graphical interface allows online data visualization in addition to the option to save data and send for offline analysis. The combination of these three sensors and deep learning algorithms increases the potential of making intelligent decisions in real-time, which enhances the quality of remote healthcare monitoring. It enables collecting medical data, tracking progress, and indicating anomalies, improving the communication between patients and clinicians, and leading to a better everyday quality of life in the end-user community.

II. Materials and Methods

In general, home is an uncontrolled environment, since it is not usually an instrumented place and there is no health professionals to monitor the patients. The instrumentation of the patient's home is a crucial stage of remote health monitoring, which allows identifying the place in the house at which the patient is in and presuming which activity he/she is performing. Since more than one person may live in the house, the environment instrumentation must be able to identify multiple people performing simultaneous movements. The proposed Opto-electronic integrated Smart Home has six regions: entrance, chair, bathroom, bedroom, bed and, desktop. Figure 1 summarizes the Opto-electronic integrated, AI-enabled Smart Home approach proposed in this paper.

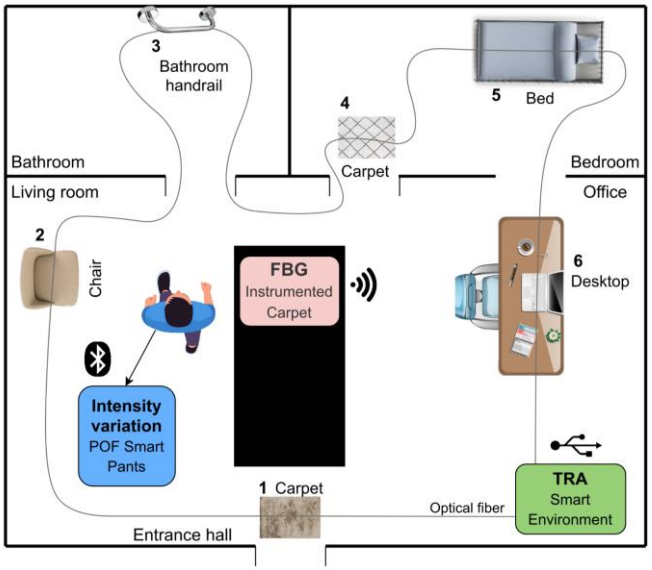

Fig. 1. Schematic representation of the proposed Opto-electronic integrated Smart Home.

A. Distributed optical fiber sensors for remote monitoring

As previously presented in [34], it is possible to identify multiple simultaneous disturbances in a TRA-based sensor using deep learning techniques. Notable advantages in using this technique include the lower cost by comparing to other distributed systems and the simple acquisition system. To that extent, a NP-doped silica optical fiber is positioned along the proposed Smart Home in strategic regions that result in the assessment of the patient location inside the environment.

The NP-doped fiber is fabricated using the Modified Chemical Vapor Deposition (MCVD) process, where a standard solution doping incorporates the magnesium (Mg) ions for the formation of the Mg-silicate nanoparticles in conjunction with the erbium ions dispersed in an ethanol solution to obtain the doping solution [35]. To increase the refractive index of the NP-doped optical fiber, germanium and small amounts of phosphorus, which result in nanoparticles with diameters smaller than 100 nm [36].

The NP-doped fibers are applied in the TRA configuration, where a broadband optical source centered at 1550 nm with a bandwidth of 60 nm (SLED, DL-BP1-1501A, Ibsen Photonics, Farum, Denmark) is connected to Port 1 of the optical circulator. The Port 2 of the circulator is connected to the NP-doped optical fiber, which has a photodetector (GT322D, Go4fiber, Hong Kong, China) at the other end of the fiber to acquire the transmitted optical power. In addition, the reflected optical power is acquired by another photodetector (GT322D, Go4fiber, Hong Kong, China) connected to the Port 3 of the optical circulator. Thus, the transmitted and reflected optical powers are analyzed as a function of mechanical perturbations in the NP-doped optical fiber. In this case, there is a proportional variation on the transmitted and reflected optical powers as function of the force and location (along the optical fiber) of the mechanical perturbation. Figure 2 presents a schematic representation of the TRA setup.

It is important to mention that Figure 2 also presents the representation of the signal processing approach, which is based on a feedforward neural network (FFNN) for the data classification. To that extent, the NP-doped fiber is positioned in the smart environment and the mechanical perturbations (of different amplitudes) are applied in 6 predefined points on the optical fiber. Tests with different combinations of force and location as well as multiple locations are performed. The data are divided into training and testing in an 80/20 ratio. In addition, the input data, i.e., transmission and reflection optical powers are normalized in the range of –1 to 1 to provide the normalized data for the neural network. The accuracy and loss of the model are evaluated as the performance metrics of the proposed model. After the model preparation, the sensor system is used in the real application of the smart environment for the online data classification, where the proposed device is able to determine the position of the person in the environment with the additional possibility of detecting more than one person in the proposed Opto-electronic Smart Home.

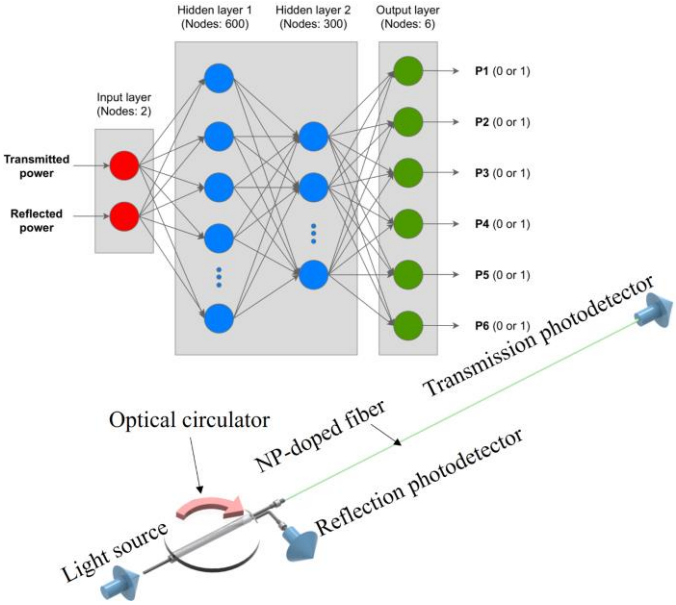

Fig. 2. Schematic representation of the TRA setup and signal processing using FFNN.

B. Instrumented Carpet based on FBG Matrix for Gait Analysis

The Instrumented Carpet is another valuable approach incorporated in the Opto-electronic Smart Home since it enables the remote monitoring of gait parameters and provides an objective evaluation of the volunteer's gait, leading to a more accurate and quick response for the clinicians. The evaluation of gait in patients after interventions or elderly with risk of fall are examples of the application of the instrumented carpet at home. Remote gait monitoring facilitates communication between patients and clinicians without the need for face-to-face medical consultation. A deep learning technique is also proposed to provide an accurate identification of disturbance location, which are useful for gait applications in smart environments.

In this setup, 10 FBGs inscribed in 2 silica fibers (5 FBGs in each fiber, separated by 20 cm) are used embedded in a rubber blanket. The FBGs were inscribed in a photosensitive single mode fiber GF1B (ThorLabs, Newton, NJ, EUA) using a 266 nm Nd:YAG pulsed laser through the phase mask technique [37]. Each fiber is positioned in one side (right or left) and the rubber blanket is used as a carpet for gait analysis. In the system setup of this Section, the FBG interrogator (HYPERION si255, Micron Optics) is connected to a router to allow wireless acquisition of FBG data that increases the portability of the proposed system through a wireless connection with the computer, which manages all data, as shown in Figure 3(a).

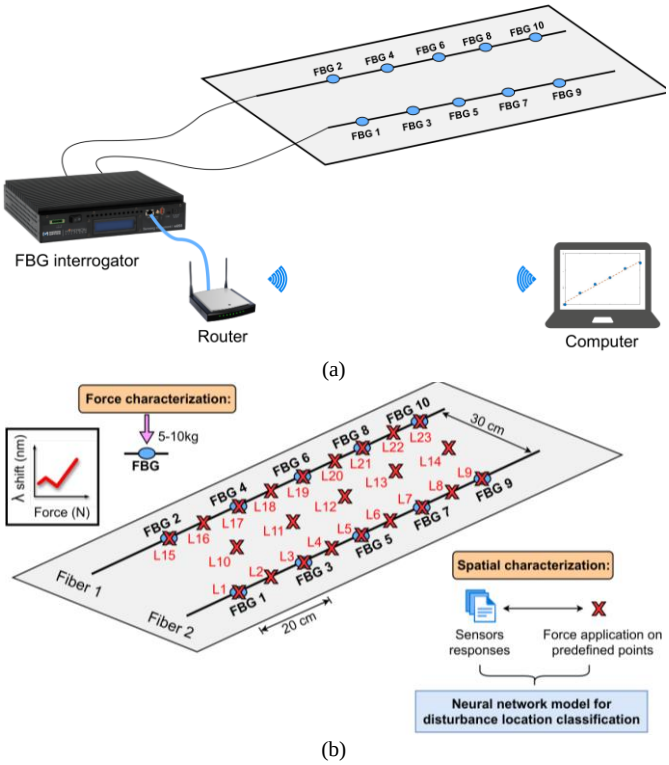

Fig. 3. (a) System setup for the FBG-based Instrumented Carpet in the Heterogeneous OFS network protocol. (b) Experimental setup of the rubber blanket-embedded FBG matrix.

Two tests are performed to evaluate the system: the force and spatial characterizations. The force characterization aims to estimate the sensitivity and the linearity of each FBG, in addition to normalize all the sensors. The force characterization of the FBGs is performed (at a constant temperature) by positioning predefined weights (5-10 kg with steps of 1 kg) on the top of each FBG. The spatial characterization aims to identify the disturbance location based on a neural network model. It consists of applying the same force on 23 predefined points and relate the sensors responses with these points to design a neural network model for classification of the disturbance location in the rubber blanket. This classification model is evaluated using accuracy and loss metrics. The setup of each characterization, as well as the FBGs incorporated in the rubber blanket are shown in Figure 3(b).

A feed-forward neural network (FFNN) is designed to perform a multi-label classification of simultaneous disturbances location on the rubber blanket. The FFNN comprises of an input layer with 10 nodes (FBG responses), two hidden layers with 600 and 300 neurons and an output layer (23 binary values). Moreover, the data are divided into training (80%) and testing (20%), and randomly permuted. The batch size is 50 and 40 epochs are used in the FFNN. The 23 locations of the rubber blanket were characterized for one volunteer by using an FFNN model. With new data, it is possible to identify the points pressed by the volunteer during his/her locomotion in the smart environment. With the foot location identification, it is possible to estimate spatio-temporal gait parameters, such as step and stride length. Moreover, kinetic parameters of the gait can be estimated by the response of the FBG sensors matrix. The ground reaction force (GRF) can be obtained by the analysis of the FBG sensors responses, which are converted to force, and represent the GRF during the gait. In addition, by analyzing the GRF of each foot it is possible to estimate single and double support duration. The FFNN model is applied on new data to classify the foot locations during the gait. Thus, parameters such as step and stride length, double support and stance phase duration, GRF are estimated by the results of the FFNN classification and the FBGs raw data.

C. Multiplexed POF smart pants

The POF Smart Pants comprises an instrumented pants with 2 POFs incorporated in the back parts of the pants (right and left sides) with a total of 60 intensity variation-based multiplexed POF sensors (30 for each leg) encapsulated by a clear urethane rubber mixture. Each sensor is fabricated by laterally coupling a light source to a lateral section, which is made by removing the cladding and part of the fiber core. The light source employed is the addressable RGB LED Strip (1 m, 60 LEDs), which allows controlling which LED turn on and the color by 1 communication bus. It leads to a more compact system using a high number of sensors. The LEDs are activated sequentially and a microcontroller FRMD-KL25Z (NXP Semiconductors, Netherlands) controls them. Four photodetectors IF-D92 (Industrial Fiber Optics, USA) are attached in each fiber end to convert the optical power into electrical power. Figure 4 presents the POF Smart Pants overview, including the sensors schematic, as shown in Figure 4(a), and the sensors system incorporated in the pants presented in Figure 4(b). A curvature characterization is performed to normalize the sensors according to their sensitivities. The curvature characterization setup, presented in Figure 4(c), consists of applying different curvatures in the sensitive region controlled by the vertical displacement between 1 mm and 5 mm. The sensors responses are related to the different curvatures and the sensors are normalized. Furthermore, the correlation between the responses of each sensor and the curvature is obtained, where the sensors sensitivities can be estimated. From the sensors sensitivities in conjunction with supervised/unsupervised machine learning approaches can also lead to the possibility classifying the activities performed by the

user.

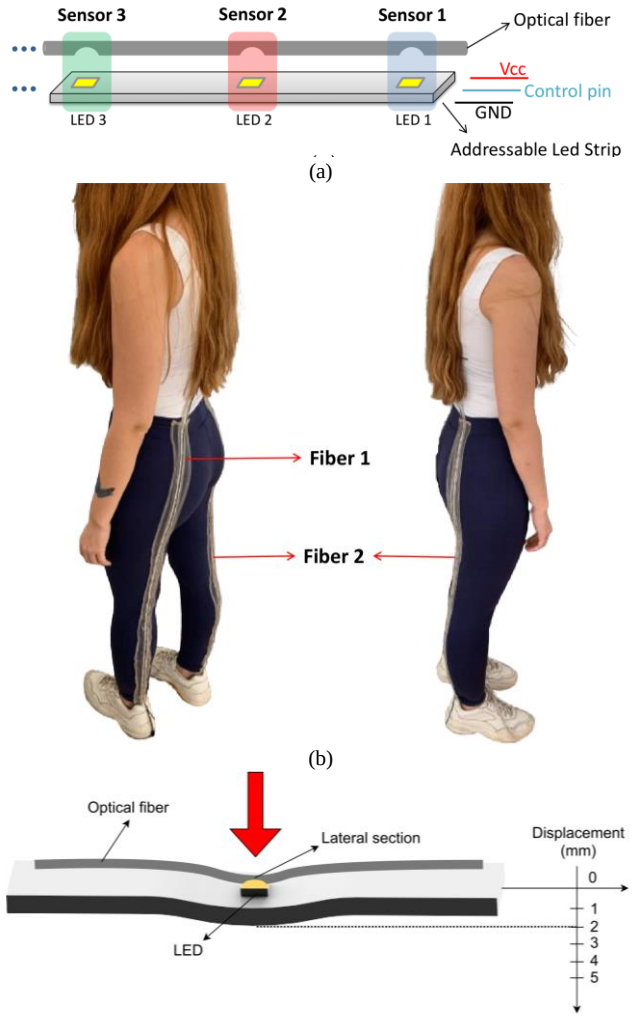

Fig. 4. Smart Pants overview. (a) Sensors system schematic. (b) Sensors system incorporated in the pants. (c) Curvature characterization setup.

D. Heterogeneous OFS Network integration

Each system included in the Smart Environment provides valuable information to the healthcare assessment. The results of each technology were presented in the previous sections. Therefore, this Section presents the integration of the systems in the Smart Environment with the simultaneous operation of the whole system. This Section aims to develop an integrated system with a heterogeneous OFS network that can provide different information about a subject (such as a patient) in real-time and remotely communicates with a clinician avoiding face-to-face consultations.

The three systems are synchronized and the data acquisition are managed by a graphical interface developed for this protocol. This interface enables online and offline acquisition. FBGs data are transmitted via Wi-Fi, the POF Smart Pants data are transmitted via Bluetooth and the TRA-based Smart Environment data are transmitted via serial communication. All data are received at same global time and operate at different clocks. The interface works with three threads that process the data from each system simultaneously at their respective clocks. The combination of all proposed systems of the Opto-electronic Smart Home leads to different layers on the remote monitoring conditions, where each layer can be obtained directly from each system or the combination between them. Figure 5(a) shows the proposed layer structure of the proposed approach, where the first layer (Layer 1) is related to the location of the patient in the Smart Home. Then, in Layer 2, the data from the POF pants that include the possibility of activities monitoring. In this case, the responses of the POF pants' sensors are used on the detection of walking, sitting and laying down activities. Finally, Layer 3 comprises of the GRF and spatio-temporal parameters of the gait are obtained when the user is in the region between the entrance carpet and the chair (Index 1 and 2 of Figure 1, obtained from the TRA responses) and the user is walking, where the walking activity is obtained from the activity classification of the POF pants. Such gait parameters are important on the remote assessment of patient gait, which is important on the balance assessment and can aid on the classification/detection of fall risk patients due to the cloud connectivity and availability of the data.

The protocol performed using all three systems that compose the Opto-electronic Smart Home includes a volunteer using the POF pants. The volunteer accesses the Smart Home in sequential order (considering the index 1 to 6 in Figure 1) and the user passes through the FBG-embedded smart carpet between index 1 and 2, i.e., between the entrance carpet and the chair. Then, the user continues the protocol from 2 to 6, which include sitting on the chair, the use of bathroom handrail, stepping on the bedroom carpet, laying on the bed and sitting on the desktop's chair. The POF pants also acquires the data from all 60 sensors during the aforementioned activities, where it is possible to evaluate the sensors responses during walking, sitting and laying down. In addition, the TRA-based sensor system acquires the data at all places, represented by the index from 1 to 6. It is important to mention that all volunteers informed consent of all participants and the tests were made in accordance with the guidelines of the national health council with the protocols approved by Research Ethics Committee through the National Commission in Research Ethics – CONEP - (Certificate of Presentation for Ethical Appreciation - CAAE: 41368820.3.0000.5542). During the protocol, the data from all systems are acquired and showed in the graphical interface. The graphical interface developed for the Smart Environment protocol using the three systems (FBG, Intensity-variation and TRA) is presented in Figure 7(b). The left part of the interface is used to connect devices and control the data acquisition (start, stop or save file for offline analysis). The central part of the interface is used for online visualization. The interface was implemented using Python and JavaScript/HTML.

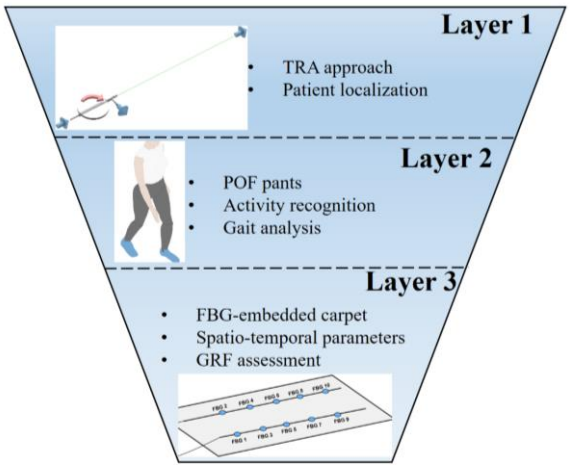

(a)

(b)

Fig. 5. (a) Schematic representation of the layer structure for remote health monitoring using the Opto-electronic Smart Home. (b) Graphical interface for data management and acquisition control.

III. Results and Discussion

A. TRA characterization results

The TRA characterization is performed by means of applying a mechanical perturbation on the regions of the NP-doped optical fiber with the same distances as the ones of index 1 to 6 of the smart home. Figure 6 presents the results of the normalized transmission and reflection optical powers of the TRA-based system for the mechanical perturbation applied at different points of the optical fiber. In addition, the transmitted and reflected optical powers are normalized as a function of the NP-doped fiber without any strain or mechanical perturbation. Thus, the application of mechanical perturbations leads to a reduction of the transmitted and reflected optical powers, as presented in Figure 6.

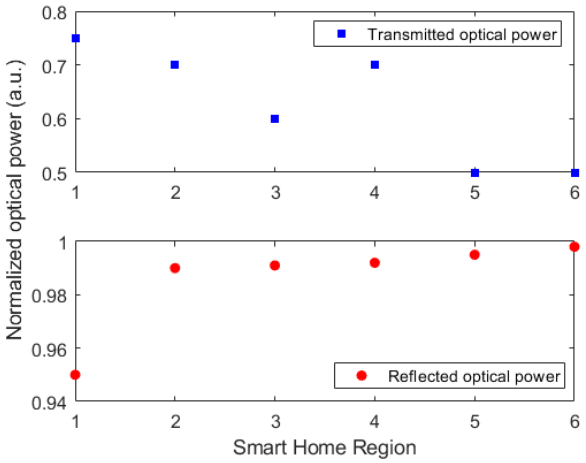

Fig. 6. Transmitted and reflected normalized optical powers for the mechanical perturbations applied at each region of the Opto-electronic Smart Home.

The results of Figure 6 indicates that the reflected optical power has direct relation with the distance between the mechanical perturbation region and the photodetector, where there is a lower reduction of the reflected optical power as the mechanical perturbation is applied farther from the photodetector used on the assessment of the reflected optical power. Therefore, it is possible to infer the position of the mechanical perturbation along the optical fiber using the transmission and reflection optical powers. However, the different forces applied in the sensor can also lead to additional optical power variations, as it is possible to observe from the transmitted optical power, where the transmission optical power variation is mainly related to the force applied on the optical fiber, as discussed and characterized in [29]. As each region of the Smart Home (indices 1 to 6) requires different forces on the optical fiber, e.g., the bathroom handrail is related to the hand pressing on the optical fiber, whereas the entrance carpet has the volunteer stepping on the optical fiber. Therefore, there is an intrinsic variation of the forces applied on the TRA-based sensor system. For this reason, the FFNN model is applied for the detection of impact localization along the NP-doped optical fiber. In the neural network training and testing, the accuracy converged to 100% with 0.01 loss in both cases, leading to a high reliable model for online identification of the patient in the Opto-electronic Smart Home. Figure 7 presents the actual and predicted results for impact identification on the NP-doped optical fiber using the TRA approach combined with the FFNN model. In this case, considering the application on the Smart Home, the results are presented as the indices 1 to 6, referring to the regions in the Smart Home (see Figure 1 for details). In addition, we dichotomize the prediction of the mechanical perturbation location, where we consider that no mechanical perturbation in a predefined region has an output 0, whereas the output is 1 when there is a mechanical perturbation on the region. Thus, the predicted values for each index are rounded to 0 or 1, leading to correct classification in all analyzed cases, as shown in Figure 7.

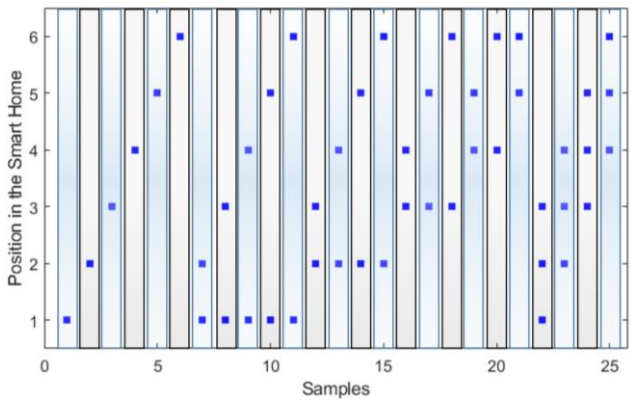

Fig. 7. Actual and predicted mechanical perturbation regions in the NP-doped optical fiber using the TRA responses in FFNN model.

B. FBG-embedded carpet characterization results

As a first step in the sensors characterization, Figure 8(a) presents the FBGs spectra of each fiber, where it is possible to observe the differences in the Bragg wavelength of each sensor. Figure 8(b)-(k) presents the results of the FBGs in the force characterization. The tests were performed at constant temperature (22°C). All sensors presented a linear relation between wavelength shift and force, with determination coefficient (R^2) higher than 0.98. The sensors' sensitivities are different, as presented in Figure 8, where such differences in the sensors sensitivities are obtained from the slope of the characterization curves. The FBG 8 presented the highest sensitivity (4.12 pm/N) among the tested ones, which is similar to FBG 2 sensitivity (3.87 pm/N), whereas the lowest sensitivities are obtained in FBGs 5 and 6 with sensitivities of 0.49 pm/N and 0.79 pm/N, respectively. The reason for this behavior is related to the positioning of the FBGs in the rubber carpet, where there are some deviations on the rubber carpet thickness (1.6±0.2 mm). The higher thickness of the carpet leads to lower force sensitivity of the sensors, whereas the lower thickness results in higher force sensitivity. Thus, the variation on the carpet thickness leads to such differences in the sensitivities of each FBG.

Since the FBGs presented different sensitivities, all the sensors are normalized by their sensitivities prior to the application in the FFNN. The results of the FFNN classification model show the high accuracy of the proposed approach, where there is the classification of the foot position based on 23 predefined positions, as shown in Figure 3(b). The accuracy value converged to 99.58% and the loss value to 0.0115. Thus, the results show the feasibility of impact detection on the FBG-embedded rubber carpet, where it is possible to estimate the spatio-temporal parameters of the gait and the ground reaction forces of the users in the FBG-embedded carpet, which are further evaluated in the Opto-electronic Smart Home implementation and validation tests.

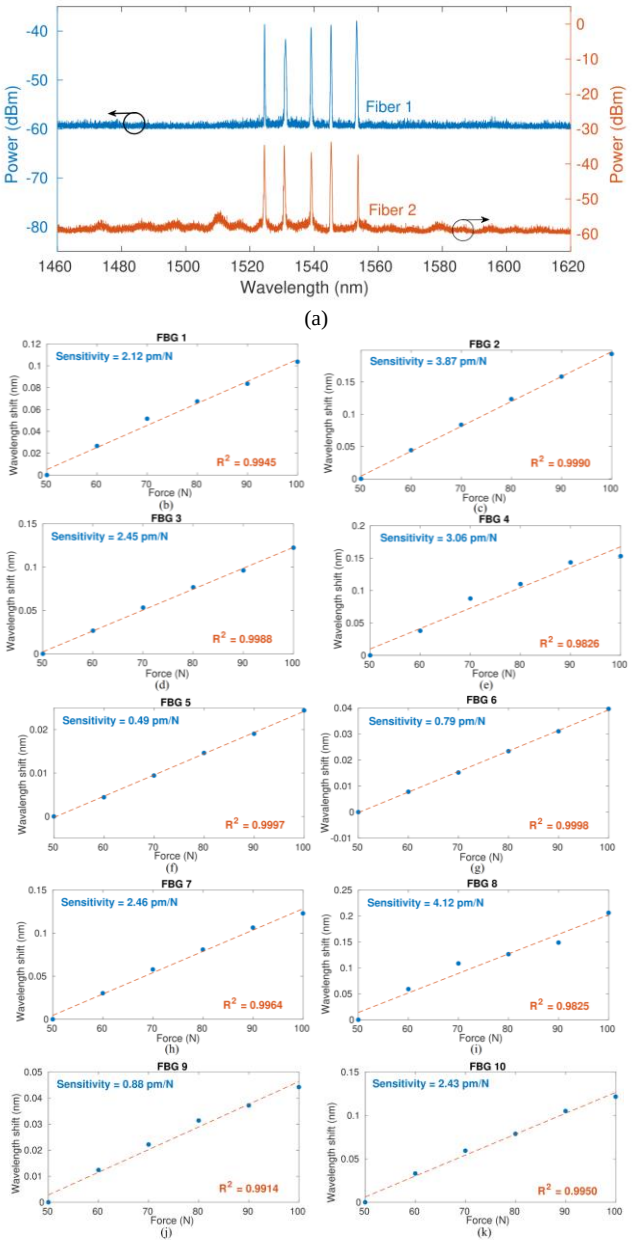

Fig. 8. (a) FBGs spectra. Top: fiber 1. Bottom: fiber 2. Force characterization of each FBG. (b) FBG 1. (c) FBG 2. (d) FBG 3. (e) FBG 4. (f) FBG 5. (g) FBG 6. (h) FBG 7. (i) FBG 8. (j) FBG 9. (k) FBG 10.

C. POF pants characterization results

Results of the curvature characterization showed different sensors sensitivities. This difference is related to the manufacturing process, which eventually presents minor differences between sensors, since lateral section parameters (length and depth) as well as the distance between the LED and the optical fiber's lateral section may have small differences for each sensor. All the sensors responses in the characterization are linear fitted (R^2 higher than 0.9). Figure 9 presents the sensitivities (in mV/mm) of the sensors positioned in the both sides of the pants, where it is possible to observe the differences

between the sensors sensitivities. Fabrication stages such as the sensitive zone creation and the encapsulation of clear urethane rubber mixture can lead to differences between sensors, due to the low precision to achieve the same lateral section parameters and the same coupling of the sensitive zones to their respective LEDs during the encapsulation are related to the sensitivity differences between sensors. However, the differences between sensors can be solved with the sensors normalization.

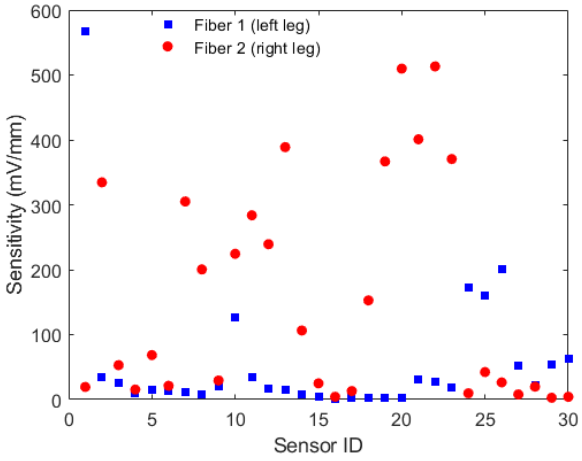

Fig. 9. Results POF pants characterization.

D. Opto-electronic Smart Home implementation

Considering the aforementioned protocol for the smart home evaluation, Figure 10 presents the results of the three systems during a protocol performance. As mentioned, each system provide an important information, which was divided considering the layer structure of Figure 5(a). Figure 10(a) shows the transmitted and reflected optical powers, indicating the places accessed by the volunteer, whereas Figure 10(b) shows the sensors' responses of the POF Smart Pants. This result led to the identification of the user's activities during the protocol. In addition, Figure 10(c) shows the responses of the activated FBGs of the Instrumented Carpet during the protocol. Since only FBG1, FBG2, FBG3 and FBG6 presented significant variation correspondent the GRF, this result indicates the path performed by the volunteer during the protocol. It is important to mention that the results are obtained in around 70 seconds of the protocol and are presented as obtained by the graphical interface and storage unit, which can be remotely assessed by health professionals for the evaluation of the patient. The results in Figure 10 also shows the synchronization of the heterogeneous sensors systems in the Opto-electronic Smart Home, where all systems are interconnected and the proposed evaluation protocol could be evaluated using the responses of each sensor system in the time-domain. Then, the sensors responses can be further processed, considering the layer structure, where Layer 1 comprises TRA-based sensors analysis, Layer 2 is related to the POF pants responses and Layer 3 is the FBG-embedded smart carpet responses for the gait parameters analysis as well as activity recognition/classification.

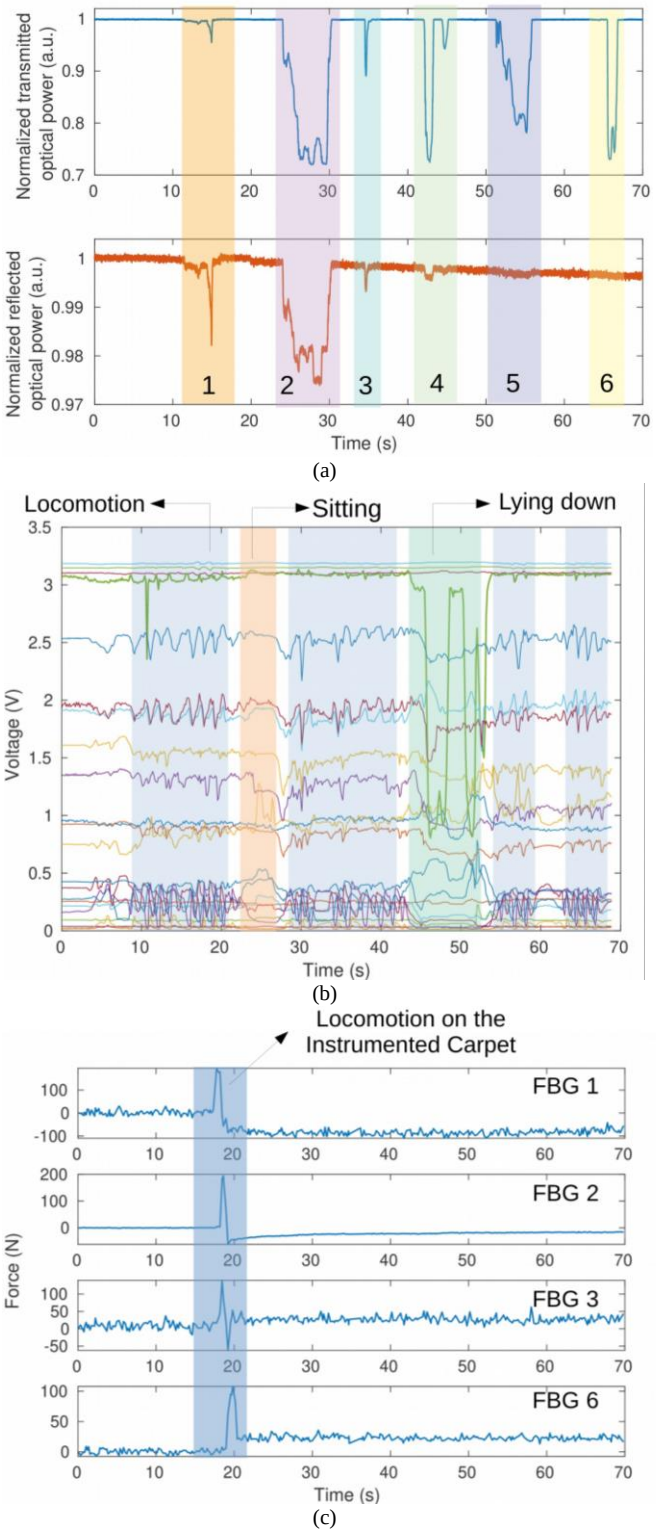

Fig. 10. Result of the Smart Environment protocol using the synchronized systems. (a) TRA-based Smart Environment. (b) POF Smart Pants. (c) FBG-based Instrumented Carpet.

Considering the Layer 1 of the division of the Opto-electronic Smart Home presented in Figure 5(a), the TRA approach is used to identify the patient position inside the smart home. Based on the results of the classification metrics and the characterization of each sensor system, the FFNN model is used

as the classifier of new data and identify the places accessed using the TRA-based approach. Figure 11 presents the results of data classification using the proposed FFNN model. As previously mentioned, the input data (reflection and transmission optical powers) are normalized in the range of -1 to 1. The output follows the same pattern presented in the TRA system characterizations, where 1 represents when a place is accessed and 0 when no place is accessed. The predicted output is the result of the FFNN model based on an input sample and corresponds to the probabilities of each class. These probabilities are rounded for accuracy estimation. The results of Figure 11 indicates the suitability of the proposed approach on the assessment of patient's position inside the smart home.

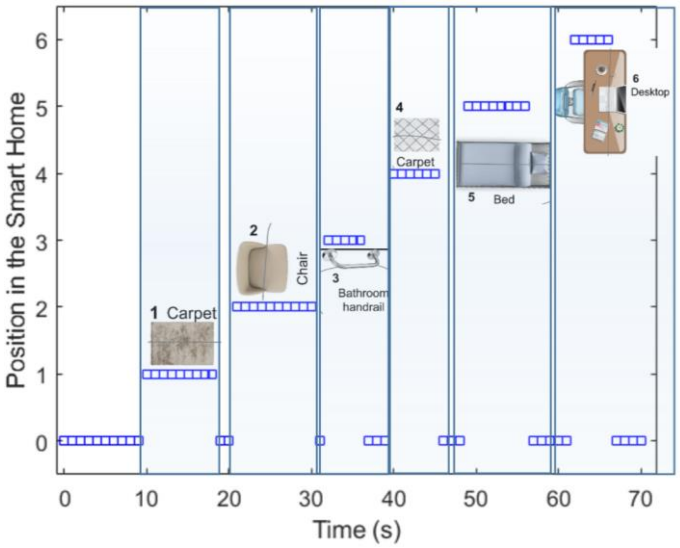

Fig. 11. Position in the Smart Home, obtained from the TRA-based system with the applied FFNN model, as a function of time.

Thereafter, the POF pants responses can lead to the possibility of activity recognition that can add more features to the patient's data obtained from the TRA-based system (Layer 1). In this case, the combination of the TRA approach and the POF pants responses can indicate not only the position of the patients inside the Opto-electronic Smart Home, but also their activities. The results in Figure 10(b) show this possibility, since it is possible to observe different trends in the sensors responses following each activity proposed in the experimental protocol. For this reason, the combination of the sensors data with machine learning approaches result in real time activity recognition. To that extent, Figure 12(a) shows the cluster of points, where each point is related to the normalized optical power considering 2 sensors at same position, but one sensor on the left side of the POF pants and the other on the right side. Such results indicate the feasibility of detecting the activities, since such differences were obtained using only two sensors. Thus, it is expected that the use of the other sensors in the POF pants can increase the accuracy and reliability of the activity classification. In addition, such high number of sensors can also indicate the possibility of additional evaluations of the patient's conditions, especially in gait analysis. Regarding the gait analysis, Figure 12(b) presents the response of two sensors located at the same position correspondent to each leg in a gait performance. This result shows the ability to identify the steps (left and right) during a gait using only two sensors. Moreover, these sensors responses allow the estimation of the cadence and other spatio-temporal gait parameters, such as the stance and swing phases, and the double support, which is explored in Layers 2 and 3 of the proposed Opto-electronic Smart Home.

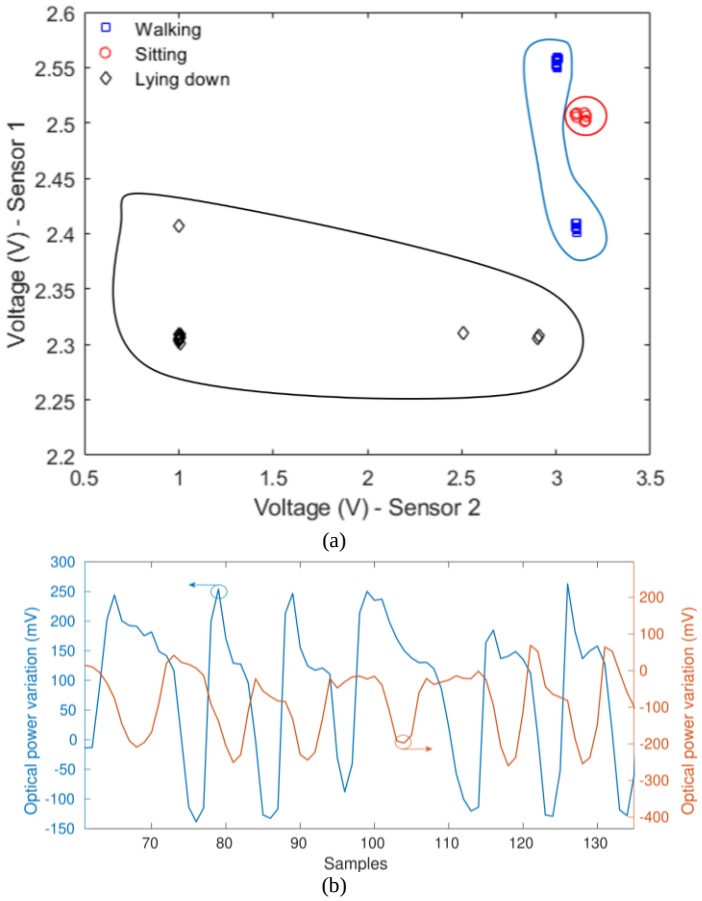

Fig. 12. (a) Responses of two contralateral sensor for the different performed activities. (b) Selected sensors during the gait performance: left and right legs.

As presented in Figure 8, the FBG sensors embedded in the smart carpet present different sensitivities in the force characterization. Differences between sensitivities are related to the FBG positioning in the carpet, which has minor differences in its thickness, leading to variations in sensors sensitivities depending on their positions in the rubber carpet. After the sensors normalization, the GRF during the gait performance was analyzed. The temporal response of each sensor is presented in Figure 13(a). The GRF data indicate the single and double support periods since there are samples in which only one sensor is pressed and samples in which two sensors are simultaneously pressed. It also leads to the evaluation of stance and swing phases of each foot. In addition, Figure 13(b) presents the temporal responses of these sensors relating them to the support moments (single or double) of two steps (left and

right) during the gait. The responses were presented using FBGs 4 and 5 as an example due to their positioning in the middle region of the carpet. It is possible to observe that the sensors responses during the transition of the foot in the gait presents characteristics that enable the identification of the gait phases. Each FBG curve consists of two different peaks. This behavior corresponds to the body load transition during the gait, i.e., the first single support (left foot) initiates with a heel strike in which the body weight is concentrated on the heel and finishes when the right foot goes to the floor and divides the body weight with the left foot. Thereafter, the double support is initiated with heel strike of the right foot while the left foot is finishing the stance phase with toe-off, and for this reason, the second peak of the left foot is lower than the first one. The double support finishes when the left foot leaves the ground, and the single support of the right foot initiates. By analyzing consecutive contralateral steps, as presented in Figure 13(b), it is possible to estimate the percentage of double support during the stance phase, commonly used in scientific literature to identify gait anomalies. The double support period indicates bilateral floor contact, but not equal load sharing [38]. In the same context, in the analysis of consecutive ipsilateral steps, it is possible to estimate the percentage of stance and swing phases' duration, also commonly used for gait assessment, as presented in Figure 13(c).

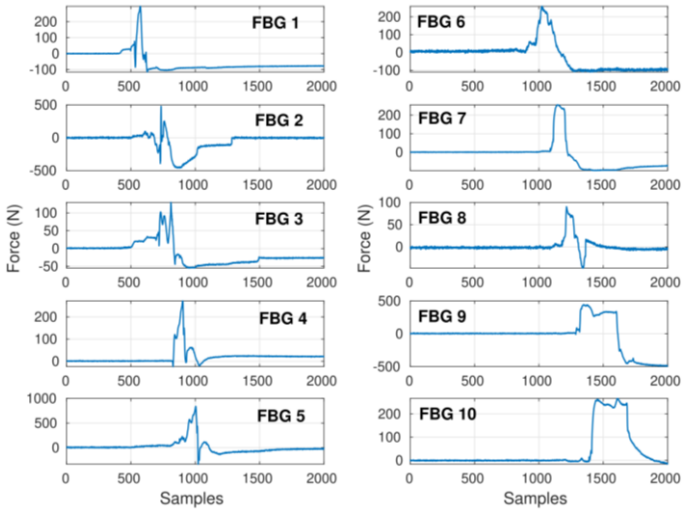

(a)

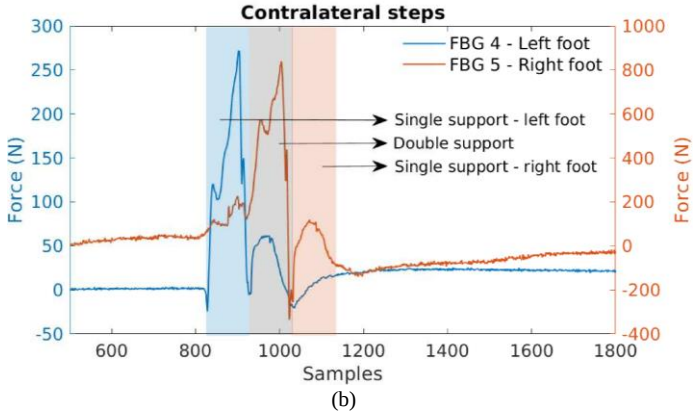

(b)

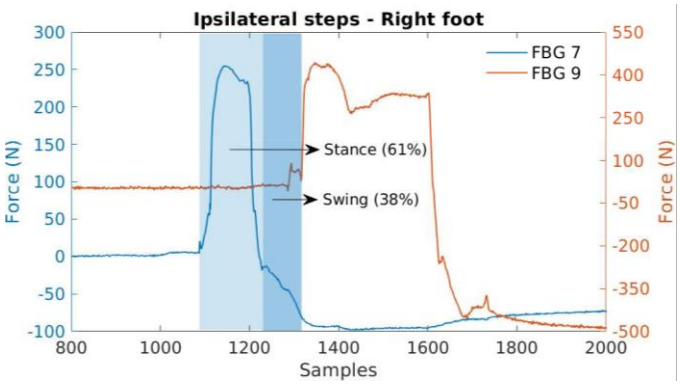

(c)

Fig. 13. (a) Sensors responses after normalization during a gait performance. (b) Sensors responses of FBG 4 and FBG 5, and the estimation of support periods (single and double) of two consecutive contralateral steps during the gait. (c) Sensors responses of FBG 7 and FBG 9 and the estimation of stance and swing phase duration during a gait cycle.

For the gait analysis, by using the FFNN model previously designed for this application, the locations in the instrumented carpet during a new gait performance were classified using new input data. Figure 14 presents the classification results in three different moments in the gait along the carpet (beginning, middle and end of the carpet) with the real output and the output predicted by the designed FFNN model. The FFNN output presents the probabilities of each class (location). Even if the probabilities are not 1, they can indicate the correct classification by using a threshold, since the locations that are not pressed always present probabilities equal to 0.

IV. Conclusions

This paper presented the integration of three sensors using different OFS techniques for simulation of the remote healthcare monitoring at home, resulting in the so-called Opto-electronic Smart Home. The three systems provide different information acquired with the different sensors systems: identification of the place where the volunteer is in the house; analysis of the user's movements, and identification of the activities; assessment of the volunteer's gait during daily activities. The system is divided into layers considering the specificity and the possibility of measuring additional parameters. Therefore, in Layer 1, the TRA-based system enable the identification of the user's position in the smart environment, whereas the results from the smart pants indicate which activity the user is performing, related to Layer 2. Furthermore, considering Layer 3, the FBG-embedded rubber carpet is in a region of the smart environment at which the GRF and spatio-temporal parameters of user's gait are acquired. Thus, the FBG-embedded carpet in the smart environment is a region at which the gait of the user is analyzed and excludes the necessity of patient transportation to clinical environment for this end. The combination of these data provides a higher level of health monitoring at home when compared with isolated systems. This can be useful for clinicians to acquire more information about patients' health, be able to diagnose the correct treatment and even anticipate health issues (specially

the gait-related ones), which result in new paradigms and possibilities of digital health and Internet of Things.

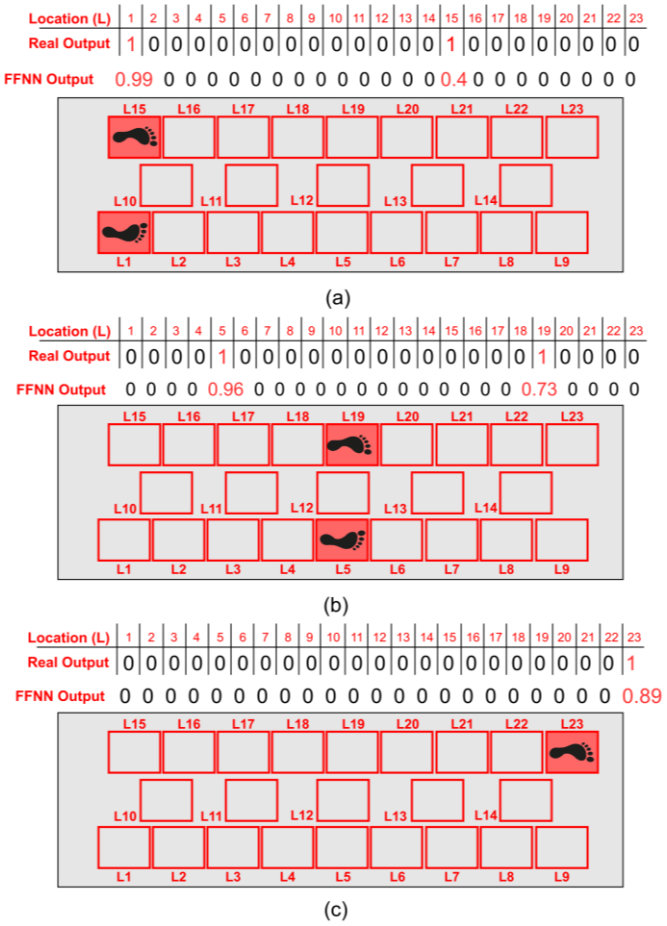

Fig. 14. Examples of the classification of locations pressed by the volunteer during a gait performance using the designed FFNN model: comparison between the real output and the FFNN output, which presents the probabilities of each class. (a) Double support at locations L1 and L15. (b) Double support at locations L5 and L19. (c) Single support at location L23.

REFERENCES

[1] G. A. Akpakwu, B. J. Silva, G. P. Hancke, and A. M. Abu-Mahfouz, "A Survey on 5G Networks for the Internet of Things: Communication Technologies and Challenges," *IEEE Access*, vol. 6, pp. 3619–3647, 2017, doi: 10.1109/ACCESS.2017.2779844.

[2] A. Ahad, M. Tahir, and K. L. A. Yau, "5G-based smart healthcare network: Architecture, taxonomy, challenges and future research directions," *IEEE Access*, vol. 7, pp. 100747–100762, 2019, doi: 10.1109/ACCESS.2019.2930628.

[3] S. Sicari, A. Rizzardi, and A. Coen-Porisini, "5G In the internet of things era: An overview on security and privacy challenges," *Comput. Networks*, vol. 179, 2020, doi: 10.1016/j.comnet.2020.107345.

[4] P. P. Jayaraman, A. R. M. Forkan, A. Morshed, P. D. Haghighi, and Y. Bin Kang, "Healthcare 4.0: A review of frontiers in digital health," *Wiley Interdiscip. Rev. Data Min. Knowl. Discov.*, vol. 10, no. 2, pp. 1–23, 2020, doi: 10.1002/widm.1350.

[5] M. H. Abidi, M. K. Mohammed, and H. Alkhalefah, "Predictive Maintenance Planning for Industry 4.0 Using Machine Learning for Sustainable Manufacturing," *Sustain.*, vol. 14, no. 6, 2022, doi: 10.3390/su14063387.

[6] L. Romeo, A. Petitti, R. Marani, and A. Milella, "Internet of robotic things in smart domains: Applications and challenges," *Sensors (Switzerland)*, vol. 20, no. 12, pp. 1–23, 2020, doi: 10.3390/s20123355.

[7] H. E. Froehlich, A. Smith, R. R. Gentry, and B. S. Halpern, "Offshore aquaculture: I know it when I see it," *Front. Mar. Sci.*, vol. 4, no. MAY, pp. 1–9, 2017, doi: 10.3389/fmars.2017.00154.

[8] D. De, P. Bharti, S. K. Das, and S. Chellappan, "Multimodal wearable sensing for fine-grained activity recognition in healthcare," *IEEE Internet Comput.*, vol. 19, no. 5, pp. 26–35, 2015, doi: 10.1109/MIC.2015.72.

[9] M. F. Domingues *et al.*, "Insole Optical Fiber Sensor Architecture for Remote Gait Analysis—An e-Health Solution," *IEEE Internet Things J.*, vol. 6, no. 1, pp. 207–214, Feb. 2019, doi: 10.1109/JIOT.2017.2723263.

[10] S. Majumder, T. Mondal, and M. Deen, "Wearable Sensors for Remote Health Monitoring," *Sensors*, vol. 17, no. 12, p. 130, Jan. 2017, doi: 10.3390/s17010130.

[11] S. Abdulmalek *et al.*, "IoT-Based Healthcare-Monitoring System towards Improving Quality of Life: A Review," *Healthcare*, vol. 10, no. 10, p. 1993, Oct. 2022, doi: 10.3390/healthcare10101993.

[12] B. M. Quandt, L. J. Scherer, L. F. Boesel, M. Wolf, G. L. Bona, and R. M. Rossi, "Body-Monitoring and Health Supervision by Means of Optical Fiber-Based Sensing Systems in Medical Textiles," *Adv. Healthc. Mater.*, vol. 4, no. 3, pp. 330–355, 2015, doi: 10.1002/adhm.201400463.

[13] S. Selvaraj and S. Sundaravaradhan, "Challenges and opportunities in IoT healthcare systems: a systematic review," *SN Appl. Sci.*, vol. 2, no. 1, pp. 1–8, 2020, doi: 10.1007/s42452-019-1925-y.

[14] A. Leal-Junior *et al.*, "Polymer optical fiber-based integrated instrumentation in a robot-assisted rehabilitation smart environment: A proof of concept," *Sensors (Switzerland)*, vol. 20, no. 11, pp. 1–16, 2020, doi: 10.3390/s20113199.

[15] C. Broadway, R. Min, A. G. Leal-Junior, C. Marques, and C. Caucheteur, "Toward Commercial Polymer Fiber Bragg Grating Sensors: Review and Applications," *J. Light. Technol.*, vol. 37, no. 11, pp. 2605–2615, 2019, doi: 10.1109/JLT.2018.2885957.

[16] A. G. Leal-Junior and C. Marques, "Diaphragm-Embedded Optical Fiber Sensors: A Review and Tutorial," *IEEE Sens. J.*, vol. 21, no. 11, pp. 12719–12733, Jun. 2021, doi: 10.1109/JSEN.2020.3040987.

[17] A. G. Leal-Junior, C. A. R. Diaz, L. M. Avellar, M. J. Pontes, C. Marques, and A. Frizera, "Polymer Optical Fiber Sensors in Healthcare Applications: A Comprehensive Review," *Sensors*, vol. 19, no. 14, p. 3156, Jul. 2019, doi: 10.3390/s19143156.

[18] D. Li, "5G and intelligence medicine—how the next generation of wireless technology will reconstruct healthcare?," *Precis. Clin. Med.*, vol. 2, no. 4, pp. 205–208, 2019, doi: 10.1093/pcmedi/pbz020.

[19] Z. Zhao, Z. Yu, K. Chen, and Q. Yu, "A Fiber-Optic Fabry-Perot Accelerometer Based on High-Speed White Light Interferometry Demodulation," *J. Light. Technol.*, vol. 36, no. 9, pp. 1562–1567, 2018, doi: 10.1109/JLT.2017.2783882.

[20] A. Leal-Junior, A. Frizera, and C. Marques, "A fiber Bragg gratings pair embedded in a polyurethane diaphragm: Towards a temperature-insensitive pressure sensor," *Opt. Laser Technol.*, vol. 131, no. February, p. 106440, 2020, doi: 10.1016/j.optlastec.2020.106440.

[21] A. G. Leal-Junior, A. Frizera, C. Marques, and M. J. Pontes, "Viscoelastic features based compensation technique for polymer optical fiber curvature sensors," *Opt. Laser Technol.*, vol. 105, pp. 35–40, 2018, doi: 10.1016/j.optlastec.2018.02.035.

[22] Z. Ding *et al.*, "Distributed Optical Fiber Sensors Based on Optical Frequency Domain Reflectometry: A review," *Sensors*, vol. 18, no. 4, p. 1072, 2018, doi: 10.3390/s18041072.

[23] A. Leal-Junior, L. Avellar, V. Biazi, M. S. Soares, A. Frizera, and C. Marques, "Multifunctional flexible optical waveguide sensor: on the bioinspiration for ultrasensitive sensors development," *Opto-Electronic Adv.*, vol. 0, no. 0, pp. 210098–210098, 2022, doi: 10.29026/oea.2022.210098.

[24] C. Massaroni, P. Saccomandi, and E. Schena, "Medical smart textiles based on fiber optic technology: An overview," *J. Funct. Biomater.*, no. April, pp. 204–221, 2015, doi: 10.3390/jfb6020204.

[25] A. Leal-Junior and C. Marques, "Optical Fiber-Integrated Smart Structures: Towards Transparent Devices for Healthcare 4.0," *IEEE Instrum. Meas. Mag.*, vol. 24, no. 5, pp. 41–49, 2021, doi: 10.1109/MIM.2021.9491005.

[26] L. Schenato, "A Review of Distributed Fibre Optic Sensors for Geo-Hydrological Applications," *Appl. Sci.*, vol. 7, no. 9, p. 896, Sep.

2017, doi: 10.3390/app7090896.

[27] M. Silveira *et al.*, "Transmission–Reflection Analysis in high scattering optical fibers: A comparison with single-mode optical fiber," *Opt. Fiber Technol.*, vol. 58, no. June, p. 102303, 2020, doi: 10.1016/j.yofte.2020.102303.

[28] D. Tosi, C. Molardi, and W. Blanc, "Rayleigh scattering characterization of a low-loss MgO-based nanoparticle- doped optical fi ber for distributed sensing," *Opt. Laser Technol.*, vol. 133, no. August 2020, p. 106523, 2021, doi: 10.1016/j.optlastec.2020.106523.

[29] A. G. Leal- *et al.*, "Wearable and Fully-Portable Smart Garment for Mechanical Perturbation Detection with Nanoparticles Optical Fibers," *IEEE Sens. J.*, no. c, pp. 1–1, 2020, doi: 10.1109/jsen.2020.3024242.

[30] A. G. Leal-Junior *et al.*, "Plane-by-Plane Written, Low-Loss Polymer Optical Fiber Bragg Grating Arrays for Multiparameter Sensing in a Smart Walker," *IEEE Sens. J.*, vol. 1748, no. c, pp. 1–1, 2019, doi: 10.1109/JSEN.2019.2921419.

[31] H. Li *et al.*, "Fully Photonic Integrated Wearable Optical Interrogator," *ACS Photonics*, vol. 8, no. 12, pp. 3607–3618, 2021, doi: 10.1021/acsphotonics.1c01236.

[32] A. G. Leal-Junior, C. R. Díaz, C. Marques, M. J. Pontes, and A. Frizera, "Multiplexing technique for quasi-distributed sensors arrays in polymer optical fiber intensity variation-based sensors," *Opt. Laser Technol.*, vol. 111, pp. 81–88, Apr. 2019, doi: 10.1016/j.optlastec.2018.09.044.

[33] L. Avellar, C. Stefano Filho, G. Delgado, A. Frizera, E. Rocon, and A. Leal-Junior, "AI-enabled photonic smart garment for movement analysis," *Sci. Rep.*, vol. 12, no. 1, pp. 1–16, 2022, doi: 10.1038/s41598-022-08048-9.

[34] L. Avellar *et al.*, "Transmission-Reflection Performance Analysis Using Oxide Nanoparticle-Doped High Scattering Fibers," *IEEE Photonics Technol. Lett.*, vol. 34, no. 16, pp. 874–877, 2022, doi: 10.1109/LPT.2022.3190356.

[35] W. Blanc *et al.*, "Compositional Changes at the Early Stages of Nanoparticles Growth in Glasses," *J. Phys. Chem. C*, vol. 123, no. 47, pp. 29008–29014, Nov. 2019, doi: 10.1021/acs.jpcc.9b08577.

[36] A. Veber, Z. Lu, M. Vermillac, F. Pigeonneau, W. Blanc, and L. Petit, "Nano-Structured Optical Fibers Made of Glass-Ceramics, and Phase Separated and Metallic Particle-Containing Glasses," *Fibers*, vol. 7, no. 12, p. 105, Nov. 2019, doi: 10.3390/fib7120105.

[37] R. Min *et al.*, "Inscription of Bragg gratings in undoped PMMA mPOF with Nd:YAG laser at 266 nm wavelength," *Opt. Express*, vol. 27, no. 26, p. 38039, 2019, doi: 10.1364/oe.27.038039.

[38] C. Kirtley, *Clinical Gait Analysis: Theory and Practice*. Philadelphia: Elsevier, 2006.